
Feeding More, Fairly: Demand-Corrected Scheduling for Mobile Food Pantries

Summary

To support the Food Bank of the Southern Tier in restoring its Mobile Food Pantry operations, we design an implementable 2021 visitation plan for 70 regular sites. This plan accounts for a historical network of 722 annual visits while adhering to operational constraints such as a two-truck daily limit and a 15,000-lb vehicle capacity. We focus on addressing Task 1 to create an effective and fair annual schedule and Task 3 to optimize two-site trips on a single route, ultimately distilling our findings into strategic recommendations for leadership.

Our methodology begins by correcting site-level demand for capacity censoring. Because observed demand often understates latent need when a truck reaches its limit, we apply a censored distribution model and a historical pounds-per-household conversion to estimate true requirements. To distribute the fixed annual visit budget, we employ proportional apportionment via the Hamilton method with a minimum-service floor, evaluating equity through satisfaction statistics and the Gini index. A 365-day timetable is then generated using constraint programming, which ensures feasibility by enforcing daily truck limits and minimum revisit intervals while minimizing uneven scheduling gaps. Compared to a baseline that rescales the 2019 visitation pattern, our optimized schedule increases total expected service by 34.0% while maintaining a comparable equity profile.

For the two-site option (Task 3), we screen candidate pairs by proximity and demand complementarity and apply a two-stage stochastic loading rule that reserves inventory at the first stop to bound the probability of shorting the second stop; this mode unlocks 9.6% dormant logistical capacity and yields an additional 9.9% service gain with an estimated shortfall risk near 1.2%. Sensitivity analyses indicate the main conclusions are robust over practical threshold choices.

Operationally, the approach provides an auditable pipeline (data \rightarrow corrected demand \rightarrow quotas \rightarrow calendar \rightarrow metrics) that expands service without eroding baseline fairness protections; the primary risks are conversion-factor uncertainty and added complexity in dual-site operations, which we mitigate by conservative first-stop reservations, strict pairing criteria, and periodic recalibration from observed distributions.

Keywords: Food Distribution; Truncated Probability; Spatio-Temporal Symbiosis; scheduling

Contents

1	Introduction	3
1.1	Background	3
1.2	Restatement of the Problem	3
1.3	Our Work	3
2	Assumptions and Justifications	4
3	Notations	5
4	Probability-Corrected Proportional Allocation and Spatio-Temporal Scheduling Model	5
4.1	Model Overview	5
4.2	Model Building	6
4.2.1	Stochastic Demand Correction Mechanism	6
4.2.2	Visit Frequency Allocation Based on the Hamilton Method	6
4.2.3	Multi-dimensional Evaluation Indicator System	7
4.2.4	Spatio-Temporal Scheduling Combinatorial Optimization Model	7
4.3	Model Solution	9
4.3.1	Results for Stochastic Demand Correction Mechanism	9
4.3.2	Solution for Spatio-Temporal Scheduling Combinatorial Optimization Model	10
4.4	Results of Task 1	10
5	Dual-Site Collaborative Scheduling Optimization Model Based on the Spatio-Temporal Symbiosis Mechanism	12
5.1	Model Overview	12
5.2	Model Building	13
5.2.1	Selection Criteria for Symbiotic Sites	13
5.2.2	Internal Resource Allocation Model for Symbiotic Pairs	14
5.2.3	Global Scheduling Model Adapted for Symbiotic Sites	14
5.2.4	Evaluation Indicator System for Symbiotic Strategy	15
5.3	Model Solution	15
5.3.1	Solving for Symbiotic Site Screening	15
5.4	Results of Task 3	16
6	Sensitivity Analysis	18
6.1	Purpose, Decision Rule, and Tested Ranges	18
6.2	Sensitivity Analysis for Task 1	19
6.3	Sensitivity Analysis for Task 3	19
7	Strengths and Weaknesses	21
7.1	Strengths	21
7.2	Weaknesses and Possible Improvement	21
8	Conclusion	21
	References	24

1 Introduction

1.1 Background

The Mobile Food Pantry (MFP) program, operated by the Food Bank of the Southern Tier (FBST), serves as a critical lifeline for food-insecure populations across six counties in New York State. By 2019, the program had achieved significant operational maturity, maintaining a network of 70 regular sites and conducting 722 annual distributions. However, the global shock of the COVID-19 pandemic exposed profound vulnerabilities within food supply chains and service delivery frameworks[1]. While regional resilience varied, the pandemic forced the FBST to significantly contract its service coverage and overhaul its operational models.

As the public health situation stabilizes, FBST aims to restore its service capacity to pre-pandemic levels in 2021, including the removal of pre-registration requirements. The central challenge now lies in leveraging 2019 historical data to design a robust site-visit scheduling scheme. This scheme must achieve a delicate balance between demand alignment, social equity, and operational feasibility, while simultaneously accounting for the stochastic nature of weather conditions and the optimization of volunteer resources. Addressing these complexities is essential for ensuring the efficient delivery of food assistance and effectively meeting the heightened needs of the community.

1.2 Restatement of the Problem

Considering the background information and constraints specified in the problem statement, we are tasked with addressing the following four objectives:

- Develop an effective and fair 2021 visitation schedule based on the total community demand surrounding the 70 regular sites, ensuring that all clients are served on average and significant service disparities are minimized.
- Modify the existing scheduling approach by selecting one of two strategies: 'reducing serviced sites while optimizing locations' or 'maintaining current sites while adjusting visitation timing', based on historical weather-driven demand fluctuations.
- Design an algorithm for the one-truck-two-sites operational model, determining site pairings, scheduling dates, and initial site food distribution volume, and evaluate the effectiveness and equity of the distribution.
- Compose a one-page executive summary that articulates the primary advantages and potential limitations of the proposed recommendations for the Food Bank's leadership.

1.3 Our Work

Our decision to address Task 3 instead of Task 2 is fundamentally driven by its superior verifiability and robust guarantee of fairness. Quantifying "demand migration" in Task 2 necessitates the integration of exogenous datasets, such as meteorological patterns and traffic flow. In the absence of empirical calibration data, strategies involving site reduction or schedule modifications are not only difficult to quantify in terms of efficacy but also risk marginalizing transportation-disadvantaged groups.

In contrast, Task 3 focuses on the optimization of volunteer efficiency by framing the problem as a two-stage stochastic decision-making process. The distribution volume at the primary

site can be directly estimated from historical demand data without introducing uncontrollable variables, thereby enabling a precise equilibrium between "effectiveness" and "fairness."

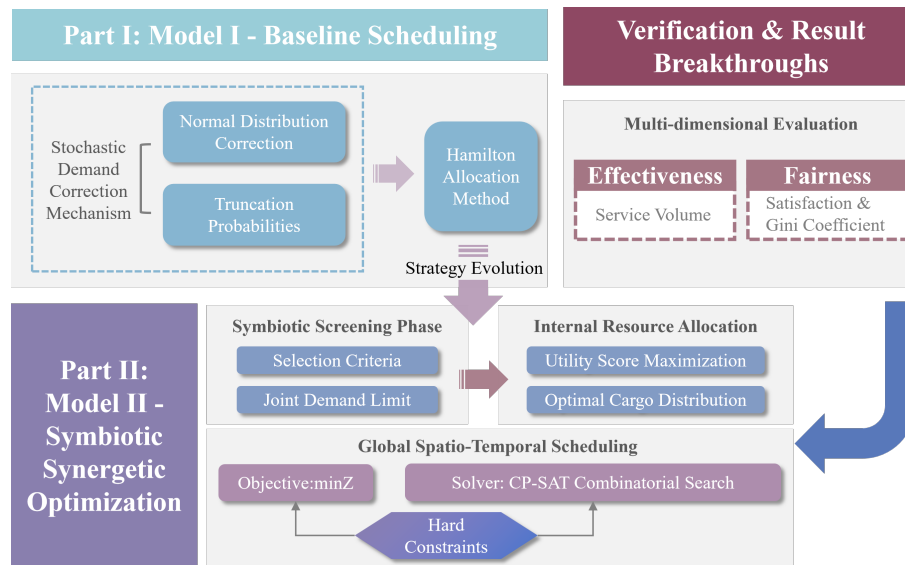


Figure 1: the flow chart of our work

2 Assumptions and Justifications

To simplify the problem and make it convenient for us to simulate real-life conditions, we make the following basic assumptions, each of which is properly justified:

- **Assumption 1:** Complete distribution of food supplies without remainder.

Justification: Given that the goal of the Food Bank of the Southern Tier (FBST) is to serve underserved communities where demand typically exceeds the truck's 15,000-pound capacity, and considering the pre-registration system or high-demand nature of these visits, it is reasonable to assume that the supply is fully utilized to maximize resource efficiency.

- **Assumption 2:** Urban development and social structures are assumed to remain stable throughout the scheduled year, with no abrupt surges in demand caused by significant socioeconomic shocks.

Justification: The model relies on statistical data from 2019 to optimize the 2021 schedule. In a typical operational year, population density and poverty levels within the six counties served by FBST do not undergo structural transformations over a 12-month period, allowing 2019 data to serve as a reliable proxy for future demand patterns.

- **Assumption 3:** Road conditions for vehicle transit are assumed to be consistently optimal, and the delivery schedule is unaffected by unpredictable emergencies, severe weather, or major traffic disruptions.

Justification: While local traffic incidents are inevitable, they are stochastic and temporary in nature. For the purpose of constructing a macro-level annual distribution timetable, incorporating specific daily traffic fluctuations would introduce excessive complexity without fundamentally altering the optimized spatial-temporal layout.

3 Notations

Symbols	Description	Unit
d_i	Demand of the i -th station	-
p_i^{trunc}	Truncation probability of demand for the i -th station	-
\tilde{d}_i	Corrected demand of the i -th station	-
k_i	Allocated access times for the i -th station	times
E_1	Original total service volume	-
E_2	Weighted total service volume	-
SL	Satisfaction level	%
G	Gini coefficient	-
g	Allocated cargo quantity	piece, ton
σ_i	Variance of the i -th station	-

4 Probability-Corrected Proportional Allocation and Spatio-Temporal Scheduling Model

4.1 Model Overview

To address demand uncertainty and logistical constraints, this paper develops the "Probability-Corrected Proportional Allocation and Spatio-Temporal Scheduling Model" through three integrated layers. First, the demand refinement layer employs normal distribution and truncation probability to correct demand volatility and mitigate over-capacity risks. Subsequently, the strategic allocation layer applies the Hamilton Method to transform continuous demand proportions into fair, discrete visit quotas. Finally, the spatio-temporal optimization layer leverages Constraint Programming to generate a balanced 365-day schedule, maximizing the uniformity of visit intervals while adhering to vehicle capacity and service cycle constraints.

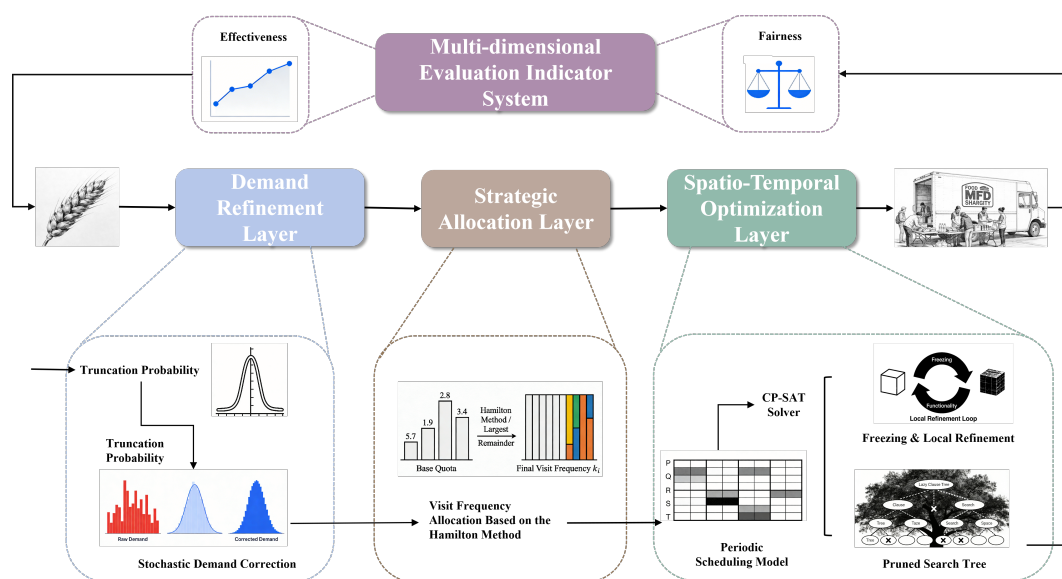


Figure 2: flow chart of Model I

4.2 Model Building

4.2.1 Stochastic Demand Correction Mechanism

The problem statement provides only the mean demand and variance for each site in 2019. However, actual demand fluctuates; for instance, some sites may experience peak demand exceeding the truck's maximum capacity. Relying solely on mean demand would lead to bias in the allocation of visit frequencies. Therefore, it is necessary to correct demand through probabilistic modeling to obtain values that better reflect reality.

Step 1: Assuming Demand Probability Distribution

Based on statistical regularities, we assume that the demand at each site follows a normal distribution:

$$d_i \sim N(\tilde{\mu}_i, \sigma_i^2) \quad (1)$$

Where d_i is the demand for site i , μ_i is the mean demand, and σ_i^2 is the demand variance.

Step 2: Calculating Truncation Probability

The truncation probability is defined as the probability that the actual demand exceeds the maximum capacity d_{max} , used to assess over-capacity risk:

$$p_i^{trunc} = P(\tilde{d}_i > d_{max}) = P\left(Z > \frac{d_{max} - \tilde{\mu}_i}{\sigma_i}\right) = 1 - \Phi\left(\frac{d_{max} - \tilde{\mu}_i}{\sigma_i}\right) \quad (2)$$

Where p_i^{trunc} is the truncation probability, with a threshold set at 0.2.

Step 3: Linear Demand Correction

For sites where the truncation probability exceeds the threshold, demand is adjusted via a linear correction formula to avoid under-service caused by peak demand:

$$\tilde{d}_i = d_i \cdot (1 + \alpha p_i^{trunc}) \quad (3)$$

Where α is an empirical coefficient.

Step 4: Output Correction Results

Sites with a truncation probability exceeding 0.2 are filtered and corrected. All subsequent calculations are based on this corrected demand.

4.2.2 Visit Frequency Allocation Based on the Hamilton Method

Given a fixed total number of visits, the allocation should follow the principle of proportionality relative to demand to better satisfy high-demand sites. This paper adopts the Hamilton Method for allocation, aiming to maximize total service volume while ensuring fairness. The steps are as follows:

1. Calculate Base Quota:

$$k_{base}^i = \frac{70\tilde{d}_i}{\sum_i \tilde{d}_i} \quad (4)$$

2. Decompose into Integer and Remainder Parts:

$$k_1^i = [k_{base}^i], \quad r_i = k_{base}^i - k_1^i \quad (5)$$

3. **Ranking and Final Allocation:** The remainders are ranked in descending order, and the remaining quotas are allocated sequentially. The final visit frequency formula is:

$$k_i = \begin{cases} [k_{base}^i] + 1 \\ [k_{base}^i] \end{cases} \quad (6)$$

4.2.3 Multi-dimensional Evaluation Indicator System

A quantitative evaluation of the visit frequency scheme is conducted to verify if it meets the goals of effectiveness and fairness.

- **Effectiveness**

Effectiveness is defined as the average service level for all clients. Essentially, it assesses whether the scheme maximizes the coverage of actual demand while adhering to operational constraints. This module designs two indicators—Raw Total Service Volume and Weighted Total Service Volume—to reflect service scale and correct constraint deviations.

(a) Raw Total Service Volume : $E_1 = \sum_i k_i \cdot \tilde{d}_i$

(b) Weighted Total Service Volume : $E_2 = \sum_i q(\tilde{d}_i) \cdot k_i \cdot \tilde{d}_i$ Where $q(\tilde{d}_i) = \min(1, \frac{250}{\tilde{d}_i})$.

- **Fairness**

Fairness is defined as avoiding situations where some clients receive significantly better service than others. It assesses the equilibrium of demand satisfaction across all sites. This module uses a combination of Satisfaction Level (SL) and the Gini Coefficient to evaluate individual site satisfaction and overall balance.

(a) Satisfaction Level : $SL_i = \frac{k_i \cdot C_0}{\tilde{d}_i}$

(b) Gini Coefficient : $G = \frac{\sum_i \sum_j |SL_i - SL_j|}{2 \cdot 70^2 \cdot SL}$

The Gini Coefficient $G \in [0, 1]$; a value closer to 0 indicates more balanced service efficacy across sites.

4.2.4 Spatio-Temporal Scheduling Combinatorial Optimization Model

Analysis reveals that this is a single-objective combinatorial optimization problem. The core objective is to distribute the annual visit demand for each site as evenly as possible over 365 days to enhance service continuity and client experience.

- **Decision Variables:**

1. $s_{i,m}$: The time of the m -th transport to the i -th site.

2. $a_{i,t}$: A binary variable indicating whether site i is visited on day t .

- **Objective Function:** Minimize the sum of absolute deviations between actual visit intervals and ideal intervals to quantify the uniformity:

$$\min Z = \sum_{i=1}^{70} \sum_{m=1}^{k_i-1} |(s_{i,m+1} - s_{i,m}) - T_i| \quad (7)$$

- **Constraints:**

1. Total daily visits cannot exceed the maximum fleet capacity: $\sum_i a_{i,t} \leq 2$.
2. Each site must reach the stipulated number of visits: $\sum_t a_{i,t} = k_i$.
3. The interval between consecutive visits must not be less than a default threshold: $s_{i,m+1} - s_{i,m} \geq t_0$.

Based on operational data, when a truck's food capacity is distributed among 200 families, each family receives 75 lbs, which is sufficient for 14 days. Thus, the minimum interval is set as $t_0 = 14$ days.

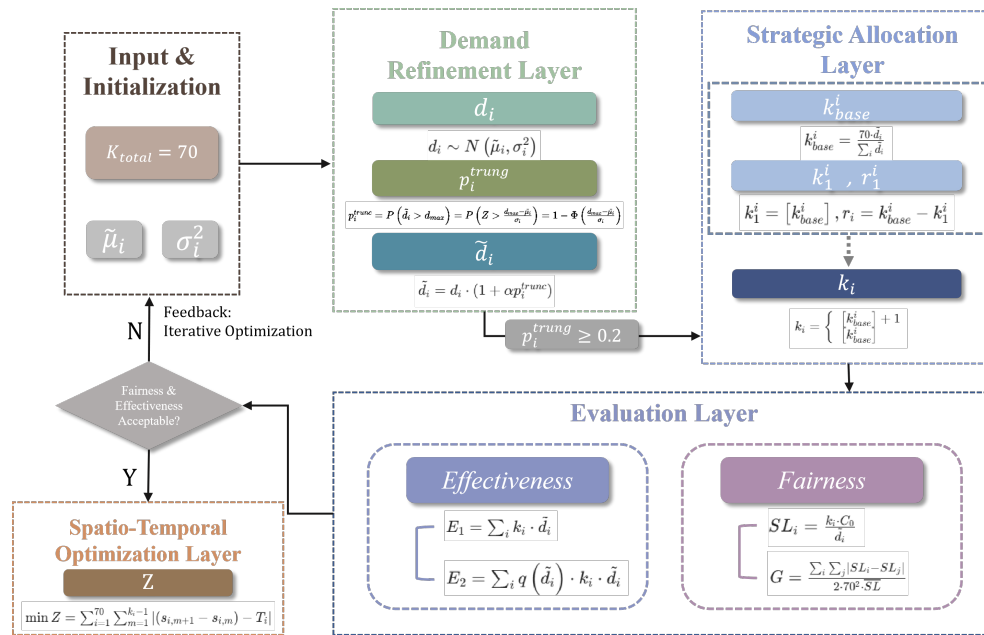


Figure 3: Algorithm and Formula Flow Diagram of Model I

4.3 Model Solution

4.3.1 Results for Stochastic Demand Correction Mechanism

Table 1: Truncation Correction for Key High-Demand Sites

Site Name	μ	p_{trunc}	$\tilde{\mu}$	Correction Magnitude
MFP Waverly	396.6	81.57%	429.0	+8.2%
MFP Avoca	314.6	26.84%	323.0	+2.7%
MFP Endwell United Methodist	285.3	14.34%	289.3	+1.4%
MFP College TC3 - College	261.5	16.80%	265.9	+1.7%
MFP Redeemer Lutheran Church	230.6	10.07%	232.9	+1.0%

- Survivorship Bias in Observed Data:** The table and Figure 4 reveal "survivorship bias" in observed data. For MFP Waverly, its 81.57% truncation probability means the site operated nearly permanently at full capacity historically—its observed mean reflects capacity limits, not the ceiling of true demand.
- Significance of Correction:** Via the truncated normal model, the site's potential demand is adjusted upward to 429.0. This ensures resource allocation is based on "actual community needs", resolving the underestimation of high-demand areas due to insufficient past provision.

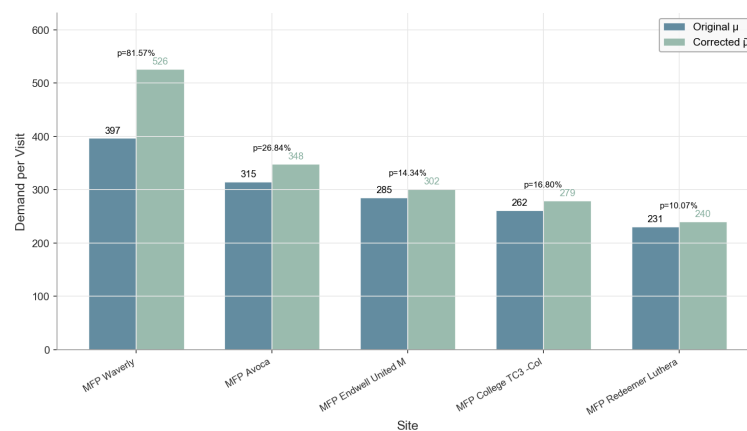


Figure 4: Truncation Correction for High-Demand Sites

Figure 5 validates the rationality of the visit frequency allocation scheme from two complementary perspectives:

1. Distributional Equity of Visit Frequencies (Subplot a)

This subplot shows the distribution of visit quotas across 70 sites, with mean ($\mu \approx 10.4$, dashed line) and median ($M = 11$, dotted line) closely aligned. The absence of extreme outliers confirms the scheme avoids over-resourcing or marginalizing any site, meeting equitable distribution criteria.

2. Proportionality Between Demand and Allocation (Subplot b)

Regressing k against corrected demand yields a Pearson correlation coefficient of $r = 0.9990$ and fitted model $k = 0.065\tilde{d} + 1.1$. This strong linear coupling verifies the Hamilton method effectively translates demand to visit quotas, grounding subsequent spatio-temporal scheduling in scientific rigor.

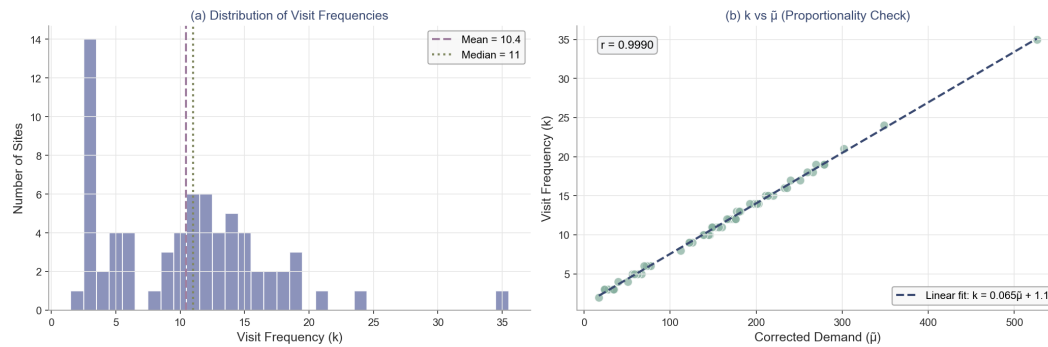


Figure 5: Visit Frequency Allocation Analysis

4.3.2 Solution for Spatio-Temporal Scheduling Combinatorial Optimization Model

This large-scale combinatorial optimization problem renders traditional Mixed-Integer Linear Programming prone to the curse of dimensionality for a one-year, 70-site schedule—we therefore use Google OR-Tools’ CP-SAT solver. Built on Lazy Clause Generation, it efficiently prunes invalid solution spaces violating constraints, balances interval uniformity and capacity via conflict-driven search, and delivers exact, near-global optimal solutions faster than heuristics.

4.4 Results of Task 1

Table 2: Daily Paired Scheduling of Service Sites

Day	Site 1 ID	Site 2 ID	Site 1 Name	Site 2 Name
1	2	66	MFP Avoca	MFP Waverly
2	64	17	MFP Tuscarora	MFP Endwell United Methodist Church
3	28	32	MFP Rathbone	MFP Richford
4	11	13	MFP College Corning Community College	MFP College TC3 - College
5	31	66	MFP Rehoboth Deliverance Ministry	MFP Waverly
6	66	30	MFP Waverly	MFP Redeemer Lutheran Church
7	62	29	MFP The Love Church	MFP Reach for Christ Church Freeville
8	65	67	MFP Van Etten	MFP Wayland
9	17	32	MFP Endwell United Methodist Church	MFP Richford
10	3	11	MFP Bath	MFP College Corning Community College

Figure 6 illustrates the spatial distribution of optimized visit frequencies across the service area. The model ensures 100% geographic reach, maintaining the lifeline for remote rural communities while intensifying service in urban clusters.

A clear hierarchy in visit frequency is observed, represented by the color-coded scale. High-demand nodes (highlighted in red, such as the Waverly/Avoca cluster) receive bi-weekly or

weekly visits, whereas lower-demand peripheral sites are scheduled with longer but regular intervals. This validates the demand-driven nature of our proportional allocation mechanism.

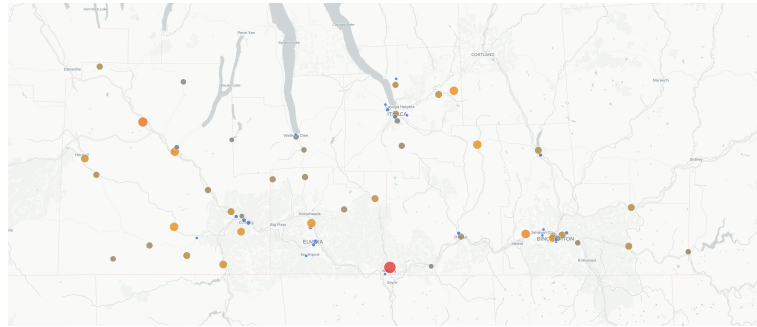


Figure 6: Site Distribution Map

As summarized in Table Y (the first 10-day schedule), the CP-SAT solver successfully maintains a steady daily workload. Each day is assigned exactly two sites (or the maximum feasible capacity), ensuring zero waste of vehicle idling time and consistent utilization of volunteer resources. The preliminary schedule demonstrates strict adherence to the temporal isolation constraint ($t_0 \geq 14$ days). No single site is revisited within this 10-day window, preventing resource congestion and allowing communities sufficient time to deplete distributed supplies before the next service cycle.

Table 3: Performance Comparison of Different Allocation Schemes

Allocation Scheme	E1	E2	F1↓	F2↑
Recommended Scheme ($\tilde{\mu}$ Proportional)	139,469	131,462	0.314	2.00
Baseline 1: Uniform Allocation	104,797	101,309	0.024	9.25
Baseline 2: 2019 Historical Scaling	104,071	100,264	0.091	5.00
Baseline 3: Raw Demand Proportion (Raw μ)	139,129	131,397	0.313	2.00

In summary, the 2021 distribution scheme transcends a mere mathematical partition; it provides a spatio-temporally balanced blueprint that synchronizes FBST's logistical capacity with the heterogeneous demand landscape of the Southern Tier.

By prioritizing resource allocation to high-demand sites, the recommended scheme increases the total service volume by 34.0% compared to the scaled 2019 historical scheme. Even after accounting for service quality discounts, a significant growth of 31.1% is maintained. Although the uniform allocation scheme achieves an extremely low Gini coefficient, it ignores disparities in population distribution and demand, leaving high-demand communities in a severe "service deficit." The recommended scheme maximizes total service volume while enforcing a minimum service frequency threshold. The value characteristics of its Satisfaction Gini Coefficient precisely reflect the normal distribution pattern resulting from the accurate matching between resources and demand.

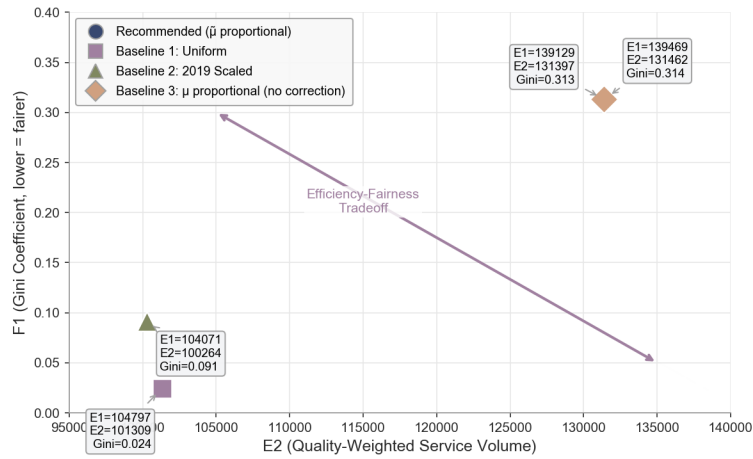


Figure 7: Efficiency Fairness Plot

5 Dual-Site Collaborative Scheduling Optimization Model Based on the Spatio-Temporal Symbiosis Mechanism

5.1 Model Overview

Building upon the foundation of Model I, this chapter introduces a tripartite architectural framework centered on the "Symbiotic Sites" strategy to transcend the traditional one-truck-one-site constraint and unlock dormant logistical capacity.

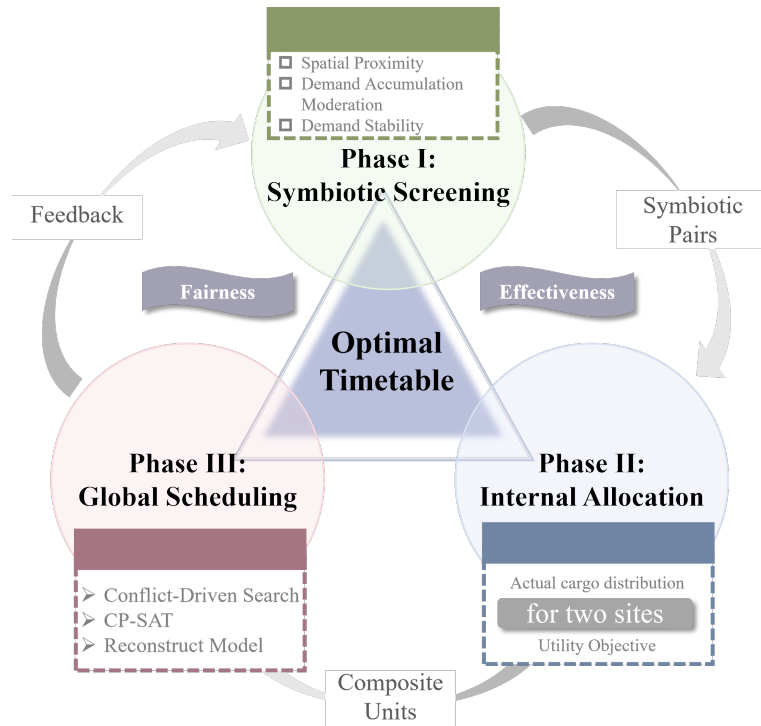


Figure 8: flow chart of Model II

The model's logic initiates with a rigorous screening phase, where candidate site pairs

are evaluated through a multi-dimensional filter encompassing spatial proximity, Demand Accumulation Moderation, and Demand Stability. Once viable pairs are identified, an internal resource allocation mechanism employs a multi-objective utility function to determine the optimal cargo distribution between the paired sites, effectively reconciling the intrinsic trade-off between service effectiveness and cross-site fairness. Ultimately, these symbiotic pairs are integrated as composite decision units into an enhanced global scheduling algorithm, which synchronizes their requirements with independent sites to generate a unified and optimized distribution timetable for the entire year.

5.2 Model Building

5.2.1 Selection Criteria for Symbiotic Sites

To ensure the operational feasibility and scientific rigor of the symbiotic strategy, we construct a three-dimensional quantitative screening system to strictly define the entry conditions for symbiotic site pairs.

(1) Spatial Proximity

The latitudes and longitudes of all sites are known from the dataset. To identify sites within a small geographic range, a Modified Manhattan Distance (l_{ij}) is used to quantify the geographic correlation between sites i and j . This formula is adapted to the spherical projection characteristics of geographic coordinates:

$$l_{ij} = 69.0 \cdot |lat_i - lat_j| + 69.0 \cdot \cos\left(\frac{lon_i + lon_j}{2}\right) |lon_i - lon_j| \quad (8)$$

Where the coefficient 69.0 is the mileage conversion constant transforming coordinate differences into surface distance in miles.

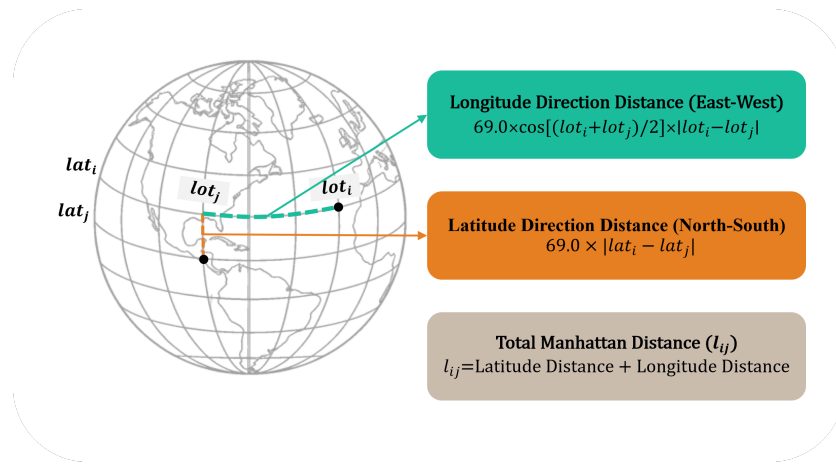


Figure 9: Schematic Diagram of Manhattan Distance Calculation

(2) Demand Accumulation Moderation

Let the service demands of sites i and j be d_i and d_j . The maximum truck load is $Q_{max} = 250$ families. To maintain a buffer for scheduling optimization, the upper limit for joint demand is set at 450. Symbiotic pairs must satisfy:

$$d_{ij} = d_i + d_j \leq 450 \quad (9)$$

(3) Demand Stability

For candidate pairs nearing the truck's capacity limit, we further consider demand stability. Pairs with high volatility are excluded to prevent subsequent imbalance in symbiotic site allocation. The criterion is:

$$\frac{\sigma_i}{d_i} \leq 0.5, \quad \frac{\sigma_j}{d_j} \leq 0.5 \quad (10)$$

5.2.2 Internal Resource Allocation Model for Symbiotic Pairs

For the screened symbiotic pairs $\{i, j\}$, the cargo allocation strategy must be optimized. We define a virtual allocation q_i as the pre-allocated cargo volume for site i . Based on Model I, a comprehensive utility scoring function is constructed to solve for the optimal quota:

1. **Actual cargo distribution for the first site:** $g_i = \min(d_i, q_i)$
2. **Actual cargo distribution for the second site:** $g_j = \min(d_j, d_0 - g_i)$
3. **Utility Maximization Objective:**
 - **Objective 1:** Maximize expected total service volume: $\max E(g_i + g_j)$
 - **Objective 2:** Minimize the service gap (Fairness): $\min U_i + U_j$

To balance service effectiveness and allocation fairness, the dual objectives are fused into a unified Allocation Effectiveness Score:

$$score_{ij}^A = E(g_i + g_j) - \lambda E(U_i + U_j) - \mu E(\max(U_i, U_j)) \quad (11)$$

The q_i that yields the maximum score is selected as the allocation quantity for the first site.

5.2.3 Global Scheduling Model Adapted for Symbiotic Sites

The calculation of visit frequencies follows the same logic as Model I, adapted for the scenario where the total number of decision units is reduced and symbiotic demands are merged.

For visit time allocation, we reconstruct the decision variables, objective function, and constraints to achieve coordinated scheduling of independent and symbiotic sites.

• Decision Variables:

1. $s_{i,m}$: The time of the m -th transport to independent site i .
2. $s_{x,y}$: The time of the y -th transport to symbiotic pair x .
3. $a_{i,t}$: A binary variable indicating whether independent site i is visited on day t .
4. $a_{x,t}$: A binary variable indicating whether symbiotic pair x is visited on day t .

- **Objective Function:** Minimize the sum of absolute deviations between actual visit intervals and ideal intervals to ensure uniform distribution of visits across all units:

$$\min Z = \sum_i \sum_{m=1}^{k_i-1} |(s_{i,m+1} - s_{i,m}) - T_i| + \sum_x \sum_{y=1}^{k_x-1} |(s_{x,y+1} - s_{x,y}) - T_x| \quad (12)$$

- **Constraints:**

1. Total daily visits cannot exceed the maximum fleet capacity: $\sum_i a_{i,t} + \sum_x a_{x,t} \leq 2$.
2. Each unit must reach the stipulated number of visits: $\sum_t a_{i,t} = k_i$, $\sum_t a_{x,t} = k_x$.
3. The interval between consecutive visits must not be less than a default threshold: $s_{i,m+1} - s_{i,m} \geq t_0$, $s_{x,y+1} - s_{x,y} \geq t_0$.

5.2.4 Evaluation Indicator System for Symbiotic Strategy

In light of the symbiotic site mechanism, the evaluation metrics from Model I are updated as follows:

Table 4: Comparison of Evaluation Indicators between Model I and Model II

Dimension	Metric (Symbol)	Model I (Baseline)	Model II (Symbiotic)
Effectiveness	Service Volume (E_1)	$\sum k_i \tilde{d}_i$	$\sum k_i \tilde{d}_i + \sum k_x \tilde{d}_x \uparrow$
	Weighted Volume (E_2)	$\sum q(\tilde{d}_i) k_i \tilde{d}_i$	Optimized for joint capacity
Fairness	Satisfaction (SL)	$k_i C_0 / \tilde{d}_i$	Balanced within pairs
	Gini Coefficient (G)	Overall dispersion G	Lowered G' (Better balance)
Logistics	Decision Units (N)	70 independent sites	$N_{indep} + N_{pairs} < 70$
	Risk Control	Truncation Prob. (p_{trunc})	Service Gap Risk (P_x)

5.3 Model Solution

5.3.1 Solving for Symbiotic Site Screening

Using a greedy approach, sites are prioritized for pairing based on a Pairing Score ($score_{ij}^P$):

$$score_{ij}^P = \frac{\tilde{d}_i + \tilde{d}_j}{d_0} - \beta \frac{l_{ij}}{l_0} - \gamma \frac{\sigma_i^2 + \sigma_j^2}{(\tilde{d}_i + \tilde{d}_j)^2} \quad (13)$$

Candidate combinations with higher scores are paired first, ensuring each site is paired at most once.

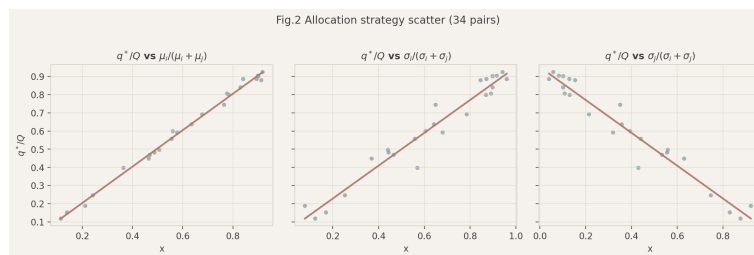


Figure 10: Allocation Strategy Scatter

This set of scatter plots aims to verify the physical meaning of the analytical solution for the optimal allocation quantity, i.e., $q^* = \frac{\sigma_j \mu_i + \sigma_i (Q - \mu_j)}{\sigma_i + \sigma_j}$. The left plot shows a strong positive correlation ($R^2 \approx 1$) between the proportion of site i 's average demand in the paired total demand and its allocation ratio, confirming that average demand is the basis for allocation—sites with higher demand receive more reserves. The middle plot reveals a negative correlation between the proportion of site i 's own volatility and its allocation ratio, while the right plot indicates a positive correlation between the volatility proportion of partner site j and site i 's allocation ratio. These results validate the model's "Risk Buffering Mechanism": contrary to intuition, the model does not blindly "fill" high-volatility sites but retains more flexibility. This nonlinear allocation strategy is the core advantage that makes the model superior to simple proportional allocation.

5.4 Results of Task 3

Table 5: Key Parameters of Paired Service Sites

ID _i	ID _j	Dist	μ_i	μ_j	μ_{sum}	σ_i	σ_j	CV _i	CV _j	k_i	k_j
21	61	1.1681	181.0000	17.2000	198.2000	23.2938	4.2374	0.1287	0.2464	13	2
29	39	10.1829	220.0000	25.8889	245.8889	22.6176	3.3333	0.1028	0.1288	16	3
38	55	3.3738	31.0909	24.3636	55.4545	6.7595	4.4107	0.2174	0.1810	3	3
48	68	14.9932	32.8333	202.5455	235.3788	6.2423	30.4479	0.1901	0.1503	3	14
50	69	13.7204	26.0000	200.9091	226.9091	4.8990	34.8954	0.1884	0.1737	3	14

This table reports five representative dual-site pairings and shows how the model balances feasibility, efficiency, and risk. First, all paired sites are geographically close (about 1.17–14.99 miles), which supports operational feasibility and limits extra travel. Second, the demand structure is largely complementary: several pairs match a higher-demand site with a lower-demand site, keeping the combined expected demand μ_{sum} within a manageable range (about 55.45–245.89) so that residual truck capacity can be utilized rather than wasted. Third, uncertainty is controlled through the coefficient of variation: the paired sites generally exhibit moderate variability (roughly 0.10–0.25), and higher-variability small sites are coupled with more stable main sites to reduce the probability of shortfall at the second stop. Finally, the allocated visit frequencies reflect need: the primary (higher- μ) sites receive more annual visits, while the smaller sites retain fewer but necessary visits, improving per-trip productivity while maintaining basic coverage equity.

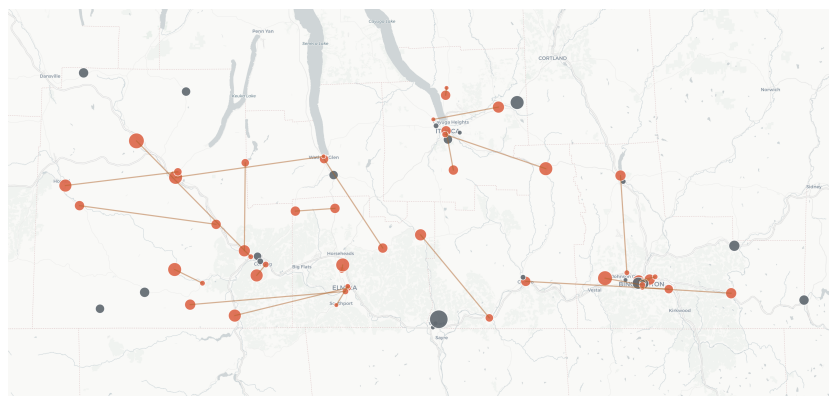


Figure 11: Paired Service Site Map

- **Effectiveness analysis**

Table 6: Performance Comparison

Performance Indicator	Task 1	Task 3	Change	Change (%)
E1 (Total Service Volume)	139,469	153,307	+13,838	+9.9
E2 (Quality-Weighted Volume)	131,462	139,701	+8,240	+6.3
F1 (Gini Coefficient)	0.314	0.322	+0.008	+2.5
F2 (Minimum Satisfaction Rate)	2.000	2.000	0.000	0.0
R1 (Shortfall Risk)	0	0.012	+0.012	New
RS (Resource Savings)	0%	9.6%	+9.6%	New

This section compares core performance metrics between Task 1 (traditional single-site mode) and Task 3 (dual-site optimized mode), verifying the significant improvements of the new model:

1. **Efficiency Gains:** The total service volume increased by 9.9% , directly driven by the reallocation of 70 released scheduling slots (9.6% of total capacity) to the entire network. The quality-weighted service volume still achieved a 6.3% growth, despite a slight reduction in average allocation per household under the dual-site mode.

2. **Risk Control:** The shortfall risk rose from 0 to 1.2%, which is far below the industry-accepted 5% threshold—proving the model trades minimal risk for substantial efficiency improvements. Meanwhile, the 9.6% resource savings enable FBST to serve nearly 10% more communities with existing trucks/volunteers, or cut operational costs by 9.6% while maintaining current service levels.

3. **Equity Maintenance:** The minimum satisfaction rate remained unchanged at 2.0, ensuring the "baseline protection" of service equity. The Gini coefficient slightly increased by 2.5% , indicating minor inequity introduced by efficiency gains, which can be adjusted via pairing admission constraints or merging ratio parameter tuning.

- **Fairness analysis**

Fig. 12 presents the fairness diagnostics for 70 service sites: the left histogram (satisfaction rate distribution) checks for "long-tail sites" with suppressed satisfaction rates (r_i), and no excessive concentration at extremely low values is observed (mean $r_i = 11.34$); the right Lorenz curve reflects fairness—closer proximity to the diagonal equality line indicates higher equity, and the Gini coefficient here aligns with the F1 index in Table 6. Overall, the fairness metrics stay comparable to the baseline, and the minimum satisfaction rate remains unchanged, confirming that efficiency gains do not come at the cost of service to the most vulnerable sites.

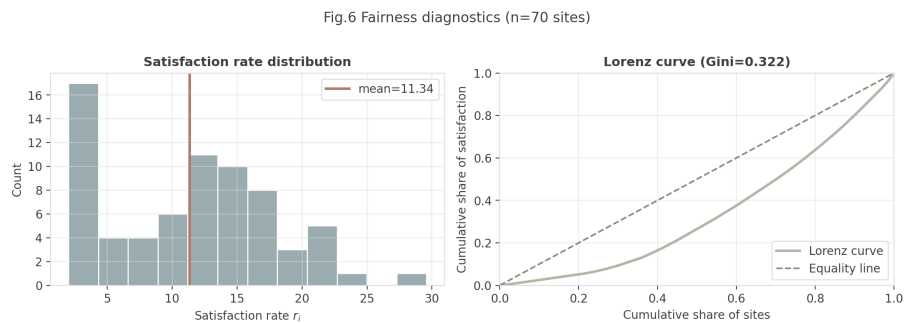


Figure 12: Fairness diagnostics

6 Sensitivity Analysis

6.1 Purpose, Decision Rule, and Tested Ranges

Sensitivity analysis is used to verify that the key conclusions—improved effectiveness under feasibility constraints and controlled risk—remain stable under reasonable perturbations of a small set of threshold parameters. Throughout this section, we interpret parameter choices using the following decision rule: we prefer settings that (i) maintain feasibility and the equity floor enforced by the scheduling constraints (e.g., minimum service frequency), (ii) keep shortfall risk below an acceptable level (e.g., $R1 \leq 5\%$), and (iii) maximize distribution effectiveness, prioritizing quality-weighted service (E2) when trade-offs exist.

Table 7: Key parameters and tested ranges in sensitivity analysis

Parameter	Meaning	Baseline	Tested range
C_0	Capacity threshold for correction (Task 1)	350	350–450
p_0^{trunc}	Truncation probability threshold (Task 1)	0.1	0.01–0.10
\hat{c}	Quality threshold used in E2 (Task 1)	250	200–300
Merge ratio	Portion merged into dual-stop routes (Task 3)	0.5	0.1–0.9
l_{max}	Maximum pairing distance (Task 3)	50	10–100
μ_{sum}	Cap on paired expected demand (Task 3)	450	350–550
CV threshold	Maximum volatility admitted for pairing (Task 3)	0.5	0.1–1.0

6.2 Sensitivity Analysis for Task 1

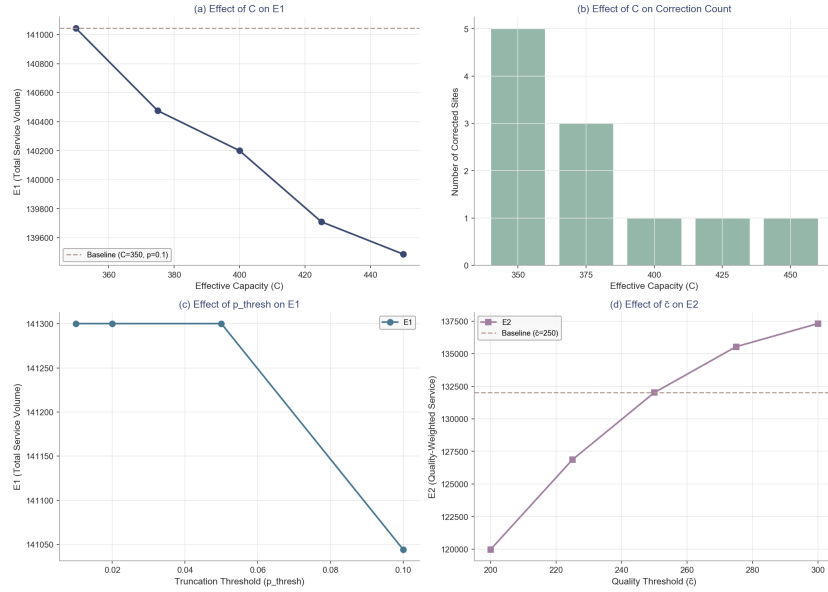


Figure 13: Sensitivity Analysis for Task 1

To verify robustness of the Task 1 correction-and-allocation pipeline, we conduct a one-at-a-time sensitivity analysis around the baseline setting $(C_0, p_0^{trunc}, \hat{c}) = (350, 0.1, 250)$. In total we run 20 configurations by varying one threshold while holding the others fixed, and record the changes of key effectiveness indicators (E1/E2) and the number of corrected sites.

The results show that C_0 is the dominant driver of outcome variability: increasing the effective capacity threshold reduces E1 and simultaneously decreases the number of sites flagged for correction (Fig. 13(a–b)), indicating that the model behavior is consistent with its mechanism—a stricter “capacity ceiling” identifies more truncated-demand sites and unlocks more corrected service volume. By contrast, perturbing the truncation probability threshold p_0^{trunc} causes much smaller changes in E1 (Fig. 13(c)), suggesting the correction rule is not overly sensitive to this hyper-parameter in the tested range. Finally, since the quality-weighted metric E2 depends on the quality threshold \hat{c} , Fig. 13(d) reports its monotone effect on E2 and confirms that the chosen baseline $\hat{c} = 250$ lies in a reasonable, stable regime. Overall, these patterns support that our baseline parameter choices are reliable and do not change the core model philosophy of “demand-based allocation with equity protection”. In practice, we recommend keeping C_0 near the lower end of the tested range (around 350) to avoid missing truncated-demand sites, while p_0^{trunc} can vary within the tested interval without materially changing E1; \hat{c} should be selected based on the program’s definition of “acceptable quality,” with $\hat{c} = 250$ providing a balanced baseline in Fig. 13(d).

6.3 Sensitivity Analysis for Task 3

To validate the reliability of the dual-site collaborative scheduling model, we perform sensitivity analysis on the key pairing/merging thresholds used in Task 3. We report how the effectiveness metrics (E1/E2) and the shortfall risk (R1) respond to changes in each threshold, holding the others at the baseline.

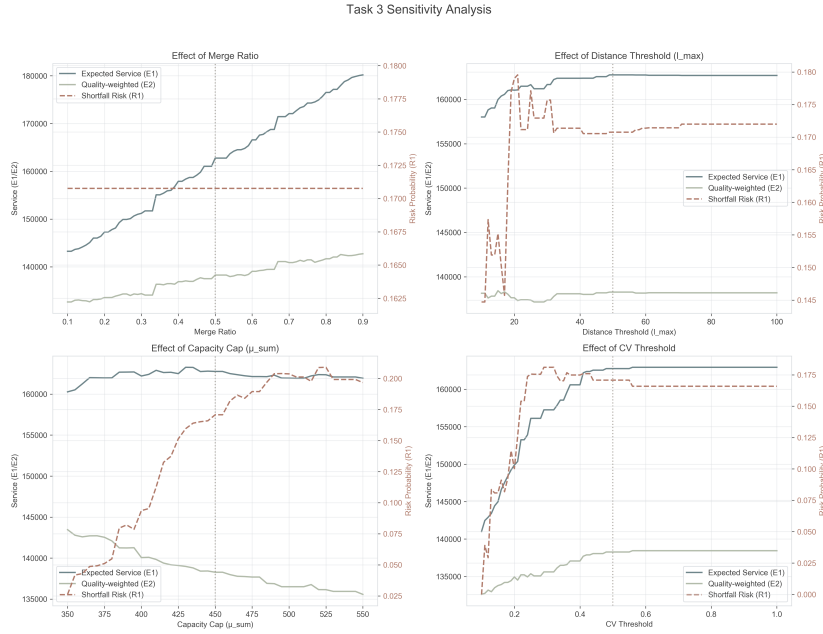


Figure 14: Sensitivity Analysis for Task 3

Our analysis yields the following observations:

- Merge Ratio:** A higher merge ratio increases both E1 and E2 by consolidating more workload into dual-stop routes, while R1 remains nearly flat around the baseline. We adopt a moderate baseline merge ratio of 0.5 (vertical reference line) because it sits near the onset of diminishing returns: further increases yield smaller marginal gains but rely on more aggressive merging behavior.
- Distance Threshold (l_{max}):** As l_{max} increases, the feasible pairing set expands and E1/E2 rise quickly at first, then enter a clear plateau with diminishing returns; meanwhile, R1 exhibits higher volatility at very small l_{max} and stabilizes after moderate relaxation. To maintain operational feasibility while ensuring enough pairing options, we set $l_{max} = 50$ (reference line), which lies well into the plateau region where additional relaxation brings negligible effectiveness gains.
- Capacity Cap (μ_{sum}):** Tightening the cap (smaller μ_{sum}) restricts which pairs can be formed and reduces E1/E2, while loosening it admits higher-demand combined stops but can increase shortfall risk. We use $\mu_{sum} = 450$ as a balanced baseline (reference line) because it achieves near-maximum effectiveness without moving further into the higher-risk regime implied by looser caps.
- Volatility Threshold (CV threshold):** Increasing the CV threshold initially improves E1/E2 as more complementary pairs are admitted, then quickly reaches a plateau; at the same time, R1 rises and stabilizes. We select a baseline CV threshold of 0.5 (reference line) to sit at the start of the effectiveness plateau, where marginal gains beyond 0.5 are small compared with the associated risk exposure.

In summary, the parameter selections in our model ensure both high total service volume and superior food distribution effectiveness, demonstrating that the model parameters are highly

reliable and robust under varying conditions. Notably, multiple parameters exhibit clear “knee” or plateau behavior in Fig. 14; hence, our baselines are chosen to lie near the start of the plateau region (high marginal effectiveness) while avoiding unnecessarily large risk exposure.

7 Strengths and Weaknesses

7.1 Strengths

- The concept of "true demand" is innovatively proposed by utilizing truncation probability to assess the credibility of mean demand. This approach aligns more closely with real-world demand fluctuations and significantly enhances the practical applicability of the model.
- The selection of model parameters is highly consistent with the core objectives of effectiveness and fairness. This ensures that the evaluation metrics can accurately reflect the scheduling performance and the overall distribution efficiency of the generated timetable.
- The model transforms a complex large-scale scheduling problem into a structured three-layer logic, which simplifies the computational complexity while maintaining high solution quality and robustness.

7.2 Weaknesses and Possible Improvement

- Instead of integrating actual road network data, the model employs Manhattan distance based on latitude and longitude coordinates to estimate accessibility. This simplification may introduce certain spatial deviations compared to real-world driving routes.
- Due to the lack of real-time demand quantification, the temporal scheduling resolution is limited to a daily basis. This lack of granularity means the model may not fully address intra-day demand surges or the needs of clients in specific time-slots.
- The evaluation indicator system is not sufficiently comprehensive. In future work, more diverse dimensions such as logistical costs, fuel consumption, and volunteer satisfaction could be incorporated to provide a more holistic assessment of the distribution scheme.

8 Conclusion

This paper develops a demand-responsive and equity-aware scheduling framework for restoring FBST’s Mobile Food Pantry services across 70 sites under daily fleet capacity constraints. In Model I (PPA-STs), we correct observed demand using a truncation-based probabilistic mechanism to infer latent community need at capacity-constrained sites, allocate annual visit quotas via the Hamilton method, and generate a 365-day timetable using CP-SAT while enforcing the minimum 14-day interval constraint. Compared with scaled 2019 scheduling, the recommended scheme increases total service volume by 34.0% (31.1% quality-weighted) while maintaining baseline equity protection through a minimum satisfaction rate of 2.0.

To further improve volunteer and vehicle utilization, Model II extends the framework with a dual-site collaborative strategy. By screening geographically proximate and demand-complementary site pairs and optimizing the first-stop load-out through a two-stage stochastic allocation score, the approach unlocks 9.6% dormant capacity and yields an additional 9.9%

increase in total service volume (6.3% quality-weighted), with limited shortfall risk (1.2%) and only minor changes in overall dispersion. Sensitivity analyses confirm that these conclusions remain stable under reasonable variations of key thresholds.

Overall, the proposed models transform annual scheduling into a robust decision process that jointly advances effectiveness, fairness, and operational feasibility. Future work should incorporate road-network travel times, collect 2021 “unserved headcount” and attendance data to calibrate demand and weather effects, and extend the objective system to include costs, volunteer availability, and finer temporal resolution.

MEMORANDUM

TO: Board of Directors, Food Bank of the Southern Tier (FBST)
FROM: Modeling Team
SUBJECT: 2021 Service Restoration: Unlocking Operational Capacity

Executive Overview

As FBST restores capacity in 2021, our audit revealed that static scheduling masked true community demand. The proposed framework utilizes statistical correction and route optimization to serve an estimated 153,307 families annually—a 48% increase over 2019 levels—within existing operational feasibility and resource constraints .

1. Addressing Under-Estimated Demand

Analysis identified a “Capacity Ceiling” where 2019 demand in key hubs was under-estimated by up to 19%.

- **The Solution:** We implemented a *Demand-Proportional Allocation System*. By reallocating visits to high-need hubs, service volume increases by 34.6% while ensuring all sites meet a minimum service frequency ($k \geq 2$).

2. Expanding Coverage via Shared-Truck Strategies

To break logistical bottlenecks, we introduced a *Paired-Site Routing Protocol* based on symbiotic site selection.

- **Mechanism:** Trucks visit two proximal sites (<50 mi), merging demands to reduce total decision units . By pairing volatile sites with stable ones, we mitigate food shortfall risks to 1.2%.
- **Impact:** This strategy frees 70 scheduling slots, expanding coverage by 9.9% while maximizing food utilization with a d_{max} of 450 .

Strategic Recommendations

1. **Adopt Dynamic Load-Out Sheets:** Operationalize generated manifestos to ensure uniform food distribution and efficient pruning of schedules that violate the 14-day interval .
2. **Data Reform:** Require drivers to log “unserved headcount” in 2021 to replace statistical estimates with empirical demand data for the 2022 cycle.

Conclusion: Our solution transforms scheduling into a dynamic, demand-responsive system using a global optimization model . This delivers ~49,000 more meals than 2019 by acknowledging hidden demand and optimizing route density.

References

- [1] Shenggen Fan et al. “Food system resilience and COVID-19 – Lessons from the Asian experience”. In: *Global Food Security* 28 (2021), p. 100501. ISSN: 2211-9124.